Influence of external magnetic fields on the growth of alloy nanoclusters

2007 J. Phys.: Condens. Matter 19 086227

(http://iopscience.iop.org/0953-8984/19/8/086227)

IOP PUBLISHING JOURNAL OF PHYSICS: CONDENSED MATTER

J. Phys.: Condens. Matter **19** (2007) 086227 (8pp) doi:10.1088/0953-8984/19/8/086227

Influence of external magnetic fields on the growth of alloy nanoclusters

M Einax[1,2], S Heinrichs[1], P Maass[2], A Majhofer[3] and W Dieterich[1]

[1] Fachbereich Physik, Universität Konstanz, D-78457 Konstanz, Germany
[2] Institut für Physik, Technische Universität Ilmenau, D-98684 Ilmenau, Germany
[3] Institute of Experimental Physics, University of Warsaw, Hoza 69, PL-00681 Warszawa, Poland

E-mail: mario.einax@tu-ilmenau.de

Received 23 October 2006, in final form 20 December 2006
Published 9 February 2007
Online at stacks.iop.org/JPhysCM/19/086227

Abstract

Kinetic Monte Carlo simulations are performed to study the influence of external magnetic fields on the growth of magnetic fcc binary alloy nanoclusters with perpendicular magnetic anisotropy. A model of the underlying kinetics is designed to describe the essential structural and magnetic properties of $CoPt_3$-type clusters grown on a weakly interacting substrate through molecular beam epitaxy. The results suggest that perpendicular magnetic anisotropy can be enhanced when the field is applied during growth. For equilibrium bulk systems a significant shift of the onset temperature for $L1_2$ ordering is found, in agreement with predictions from Landau theory. Stronger field-induced effects can be expected for magnetic fcc alloys undergoing $L1_0$ ordering.

1. Introduction

It has recently been shown that $CoPt_3$ ultrathin films and nanoclusters, grown by molecular beam epitaxy (MBE), display perpendicular magnetic anisotropy (PMA) with potential applications in high density magnetic storage media [1–3]. Previous simulations of $CoPt_3$ nanocluster growth on a weakly interacting substrate suggested that PMA originates from the combined effects of Pt surface segregation and cluster shape [4, 5]. As suggested by experiments on Co–Pt multilayer systems [6], out-of-plane CoPt bonds contribute to a magnetic anisotropy energy that tends to align the Co moments along the bond direction and thus favours PMA. When a perpendicular magnetization is induced by a magnetic field applied during growth, this type of local magnetic anisotropy energy can be expected to lead to an additional preference for out-of-plane relative to in-plane nearest neighbour Co–Pt pairs. MBE-growth of $CoPt_3$ clusters in a perpendicular field should therefore improve the formation of PMA in nanoclusters.

In order to demonstrate this latter effect we performed kinetic Monte Carlo simulations of growth within a binary alloy model, supplemented by a magnetic anisotropy energy H_A

based on Co–Pt bond contributions. Isotropic magnetic interactions, on the other hand, do not contribute in a significant way to any growth-induced structural anisotropy. Their main effect in growth simulations is a small renormalization of chemical interactions, which can be neglected. However, both types of magnetic interaction in Co–Pt and related fcc alloys can lead to an intriguing interplay between structural ordering phenomena and magnetism in samples at equilibrium [7]. We confirm this by comparing predictions of Landau theory with equilibrium Monte Carlo simulations.

2. Definition of the model

The model we consider refers to binary fcc alloys with composition AB_3. A minimal set of chemical interactions between the atoms is chosen that is consistent with the main processes during structure formation: atomic migration in different local environments, surface segregation of the majority atoms and ordering with $L1_2$ symmetry. On a semiquantitative level, these features can be reproduced by effective chemical interactions V_{AA}, V_{AB} and V_{BB} acting between nearest neighbour A or B atoms on a fcc lattice. The linear combinations $I = (V_{AA} + V_{BB} - 2V_{AB})/4$, $h = V_{BB} - V_{AA}$ and $V_0 = (V_{AA} + V_{BB})/2$ determine the bulk ordering temperature $T_0 = 1.83I/k_B$ [8], the degree of surface segregation of one atomic species and the average atomic binding energy, respectively. Following previous work [4], we adapted our model to $CoPt_3$ (A = Co, B = Pt), where $T_0 \simeq 960$ K, and Pt surface segregation is strong (nearly 100% [9]). Compatible parameters are $I = 1$, $h \simeq 4$ and $V_0 \simeq -5$, where we have used $k_B T_0/1.83 \simeq 45$ meV, corresponding to 523 K, as our energy unit. The value for V_0 describes the average binding energy for intermediate coordination numbers experienced by atoms within the growth zone near the cluster surface. The substrate (111) surface is weakly attractive with a potential $V_s = -5$ that acts on adatoms in the first layer. Compared to a Pt(111) surface with three bonds of typical strength V_0, this amounts to about one-third of the energy of a single Pt–Pt bond.

The elementary processes in our continuous time kinetic Monte Carlo algorithm, which drive the cluster growth, are (i) co-deposition of A and B atoms with a ratio of 1:3 and total flux F, (ii) hopping of atoms to vacant nearest-neighbour sites, and (iii) direct exchange of unlike nearest-neighbour atoms; one of them is an adatom with low coordination (three to five) on top of a terrace and the other one a highly coordinated atom (coordination eight to ten) underneath. Such exchange processes facilitate Pt segregation to the surface, which otherwise becomes kinetically hindered through the incoming flux. In our simulations we choose $F = 3.5$ monolayers s^{-1} (. As far as possible, other kinetic parameters are adapted from known diffusion data: jump rates for A and B atoms are of the form $\nu \exp[-(U + \max(0, \Delta E))/k_B T]$ where $\nu \simeq 8.3 \times 10^{11}$ s^{-1} is the attempt frequency, $U \simeq 5$ [10] is the diffusion barrier and ΔE denotes the energy difference before and after the jump. Direct exchange processes among pairs of unlike atoms are subjected to an increased barrier $U + U_x$ with $U_x = 5$. For more details on that model and on the choice of these parameters we refer to [4].

As explained in the introduction, PMA in $CoPt_3$ nanoclusters can be related to a structural anisotropy, expressed by the parameter

$$P = (n_{\perp}^{CoPt} - n_{\parallel}^{CoPt})/N, \tag{1}$$

which is defined in terms of the difference between numbers of Co–Pt bonds out of plane, $n_{\perp}^{CoPt}$, and in plane, $n_{\parallel}^{CoPt}$. N is the total number of atoms in the cluster. The underlying analysis [4] can in particular account for the temperature window where PMA occurs, which lies below the onset of $L1_2$ ordering. Furthermore, it provides an interpretation of PMA in terms of cluster size and shape, and the degree of Pt surface segregation. The associated magnetic model assumes a

local crystalline anisotropy energy H_A, that involves only Co moments $\boldsymbol{\mu}$ as its dominant part. Within a bond picture, each Co atom experiences an anisotropy energy that is a sum over Co–Pt bond contributions

$$-A(\boldsymbol{\mu}\cdot\boldsymbol{\delta})^2/(|\boldsymbol{\mu}||\boldsymbol{\delta}|)^2. \tag{2}$$

Here $\boldsymbol{\delta}$ is a bond vector connecting the Co atom with one of its nearest-neighbour Pt atoms, and $A \simeq 225\ \mu$eV is a parameter deduced from the interfacial part of the measured magnetic anisotropy of Co–Pt multilayers [6]. We remark that these measurements also appear to justify the bond model implied by (2), when two different interfacial orientations are compared. For (111) interfaces the anisotropy energy per surface area is found to be about twice as large as for the (100) orientation. Considering the different angles of bonds to the surface and the different packings, equation (2) can indeed reproduce this difference with one consistent value for A. Since $A > 0$, spin alignment along a Co–Pt bond is favoured. Certainly, A is small relative to the chemical interactions V_{AA}, V_{AB} and V_{BB} as well as I and h. Hence, in the absence of a magnetic field, it is justified in a first approximation to neglect (2) in simulating growth but to include it *a posteriori* in order to relate a given cluster structure to its magnetic properties.

3. Growth in external fields

However, when an external magnetic field is applied we show here that inclusion of the magnetic anisotropy energy (2) in the growth process itself leads to a small but notable change in the clusters' short range order such that PMA becomes enhanced [11]. To demonstrate this, we apply a strong field B_s perpendicular to the substrate that drives the magnetization towards saturation. Co moments $\boldsymbol{\mu}$ in (2) are then aligned along the [111] direction, which introduces an asymmetry in the probabilities for jumps that form or break CoPt bonds. For in-plane bonds, (2) gives no contribution, whereas the energy of an out-of-plane Co–Pt bond is changed from V_{AB} to $V'_{AB} = V_{AB} - \frac{2}{3}A$ in the fcc lattice geometry.

Clearly, the expected magnetic field effects on growth are small in view of the smallness of the magnetic anisotropy parameter A in (2). To obtain reliable results for the change in the structural anisotropy parameter P with and without the field, we have carried out simulations including several much larger parameters A up to $A = 1$. Note that the energy unit chosen (see above) implies that the physical value $A \sim 250\ \mu$eV corresponds to $A = 5 \times 10^{-3}$. Results for those different artificial A values will be used in turn to extract the physical change of P by interpolation.

From this analysis we first show results for the dependence $P = P(N, A)$ on cluster size N (see figure 1). All data sets referring to different A exhibit an approximate linearity in $N^{-1/3}$,

$$P(N, A) \simeq p_s(A)N^{-1/3}. \tag{3}$$

Concerning the N-dependence, this confirms that the structural anisotropy is essentially a surface effect[4]. The figure includes the case $A = 0$, represented by open symbols. These data formally correspond to zero magnetic field, because for $B = 0$ at the temperatures considered the Co moments $\boldsymbol{\mu}$ are oriented randomly so that (2) gives no contribution to P. The important observation is that $P(N, A)$ for fixed N significantly increases with A. Figure 2 explicitly shows that the behaviour of the coefficient $p_s(A)$ obtained from fits according to (3) appears to be consistent with a linear A dependence. Assuming linearity even in the limit $A \to 0$, we obtain $(p_s(A) - p_s(0))/p_s(0) \simeq 3 \times 10^{-2}$ for the physical value $A = 5 \times 10^{-3}$.

[4] Fits of data in figure 1 by straight lines and extrapolation to $N^{-1/3} \to 0$ yield in addition a non-zero bulk contribution to P which, however, is negligibly small in comparison with P values for clusters with $N \sim 10^3$ atoms.

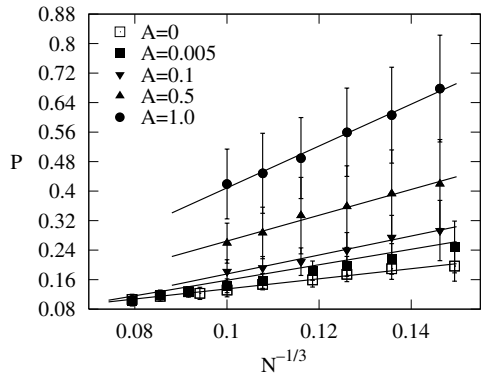

Figure 1. Simulated structural anisotropy parameter P depending on cluster size N in the presence of the saturation field B_s at temperature $k_B T = 1.2$ ($T \simeq 630$ K). Averages are performed over 20 clusters. Full lines display linearity in $N^{-1/3}$. Open symbols are equivalent to the case of zero magnetic field.

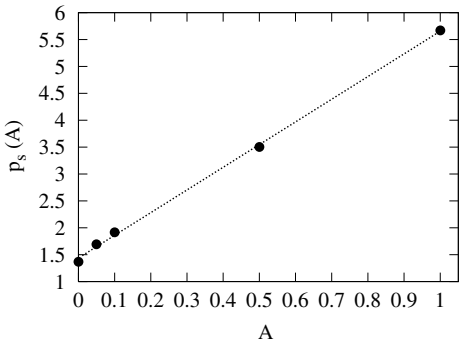

Figure 2. Coefficient $p_s(A)$ determining the structural anisotropy versus the magnetic anisotropy constant A at $T = 1.2$. Data points result from the slopes of figure 1 including the case $A = 0.05$. The dotted line is a linear fit.

This result immediately translates to the magnetic field dependence of the structural part of the total magnetic anisotropy energy E_s, which is proportional to NP. Using (3), we can write

$$E_s = K_s(B)N^{2/3}, \tag{4}$$

again with the relative change $(K_s(B_s) - K_s(0))/K_s(0) \simeq 3 \times 10^{-2}$. Thus, our main result is that the surface anisotropy constant K_s in (4) increases by about 3% when a perpendicular field of the strength of the saturation field B_s is switched on. Near $T \simeq 1$ ($T \simeq 523$ K), where the anisotropy develops its maximum [11], we obtain analogous results (not shown).

4. Interplay of structural and magnetic order in the bulk

So far we have shown that in the presence of a strong perpendicular magnetic field the anisotropy energy H_A notably affects the frozen-in structure of growing nanoclusters and thus improves PMA. Based on Landau theory, we now study the effects of external magnetic fields on the equilibrium structure of bulk systems or homogeneous films. Effects of this type are

known in principle but have been explored only for few specific materials [12, 13]. For $CoPt_3$, quantitative calculations have been performed in the past within the cluster variation method in the tetrahedron approximation [14]. Landau theory, which we use here, allows us to incorporate the magnetic anisotropy in a simple manner and helps to clarify the interrelation between different effects.

For the free energy f per Co atom in $CoPt_3$ in the presence of an external field $\mathbf{B}$ we propose the form

$$f = f_S + f_M + f_{int} - \mathbf{M} \cdot \mathbf{B}, \tag{5}$$

where $\mathbf{M} = (M_1, M_2, M_3)$ is the average magnetic moment per $CoPt_3$ unit. The first term in (5) denotes the structural free energy that describes $L1_2$ ordering without magnetic contributions [15],

$$f_S = \sum_{\alpha=1}^{3} \left(\frac{r(T)}{2} \psi_\alpha^2 + \frac{v}{4} \psi_\alpha^4 \right) + \frac{u}{4} \left(\sum_{\alpha=1}^{3} \psi_\alpha^2 \right)^2 + w \psi_1 \psi_2 \psi_3. \tag{6}$$

The structural order parameter components ψ_α, $\alpha = 1, 2, 3$, describe amplitudes for layering along one of the cubic axes α of the fcc lattice such that CoPt layers and Pt layers alternate. Superposition of these layer structures in all three directions yields the $L1_2$ structure. As usual, we set $r(T) \simeq r_0(T - T_{sp})$; $r_0 > 0$, $u > 0$, $0 < v < u$ and $w > 0$, where T_{sp} denotes the spinodal temperature. The associated ordering temperature T_0 is determined by $r(T_0) = (2/9)w^2/(3u + v)$.

The second term in (5) is the isotropic magnetic free energy, with the behaviour

$$f_M(\mathbf{M}) \sim \frac{b(T)}{2} \mathbf{M}^2, \tag{7}$$

as $\mathbf{M} \to 0$, where $b(T) \simeq b_0(T - T_C)$ and T_C denotes the Curie temperature of a disordered alloy. Finally the third term in (5), f_{int}, describes the coupling between structural and magnetic order. Retaining only the lowest-order terms allowed by symmetry, we write

$$f_{int} = \frac{c_1}{2} \left(\sum_{\alpha=1}^{3} \psi_\alpha^2 \right) \mathbf{M}^2 + \frac{c_2}{2} \sum_{\alpha=1}^{3} \psi_\alpha^2 M_\alpha^2. \tag{8}$$

For later purposes we define the Landau coefficients such that ψ_α becomes dimensionless, with $|\psi_\alpha| = \psi_{max} = 1$ for perfect structural order. Expressions (5)–(8) imply far-reaching interdependences between structural and magnetic properties. Combination with simple mean-field arguments allows us to make order-of-magnitude predictions which can be tested experimentally.

First, collecting terms in (5) which are quadratic in ψ_α, we find that in a state magnetized parallel to the [111] direction, both the spinodal and the transition temperature for $L1_2$ ordering are shifted by an amount $T_{sp}(M) - T_{sp} \simeq T_0(M) - T_0 = \Delta T_0(M)$ with

$$\Delta T_0(M) = -(3c_1 + c_2)M^2/3r_0. \tag{9}$$

To determine the c coefficients in (9) we note that a linear combination proportional to $3c_1 + c_2$ also enters the difference in Curie temperatures between disordered and ordered samples,

$$\Delta T_C(\psi_{max}) = T_C(\psi_{max}) - T_C = -(3c_1 + c_2)/b_0. \tag{10}$$

This relation is immediately obtained from (5) by requiring the terms quadratic in $\mathbf{M}$ to vanish. For the ordered samples we have set $|\psi_\alpha| \simeq \psi_{max}$, because the discontinuity ψ_0 in ψ_α at T_0 is large and Curie temperatures are considerably lower than $T_0 \simeq 960$ K. Within the same consideration the inverse magnetic susceptibility χ^{-1} develops a discontinuity at the order transition at T_0 of magnitude $(3c_1 + c_2)\psi_0^2$. Experimentally, $T_C(\psi_{max}) \simeq 400$ K, while

$\Delta T_C(\psi_{max}) \gtrsim 150$ K [14]. The reason for an increased Curie temperature in quenched, disordered samples is the increased number of Co–Co direct exchange couplings relative to the ordered state. This temperature shift already allows a rough estimate of (9). Suppose, for example, that the magnetic field is strong enough to drive the magnetic moment M to values near its saturation value M_s. Using mean field arguments, we expect that both r_0/k_B and $b_0 M_s^2/k_B$ are of order unity. Therefore the two expressions (10) and (9) should be of similar magnitude. In other words, for very strong magnetic fields $\mathbf{B} \parallel [111]$ equation (5) predicts a lowering of T_0 by about $\Delta T_{0,max} \simeq 10^2$ K in $CoPt_3$.

A further effect is worth mentioning. When the orientation of the external field is changed from [111] to [001] and $c_2 < 0$, the disordered phase develops an instability towards formation of a layered structure with $\psi_1 = \psi_2 = 0$ and $\psi_3 \neq 0$, i.e. with $L1_0$ symmetry. The corresponding transition point is increased relative to the spinodal temperature for [111] field orientation, $T_{sp}(M)$, by an amount $(2/3)|c_2|$, but will exceed $T_0(M)$ only if $|c_2|$ is sufficiently large. Otherwise this layered structure cannot form because the conventional ordering transition at $T_0(M)$ will set in before then. In $CoPt_3$ anisotropic magnetic interactions determining c_2 are weak (see below) so that this effect is unlikely to be observable.

At this point let us attempt to explicitly relate the parameters c_1 and c_2 to a specific magnetic model. For that purpose we adopt a phenomenological spin-Hamiltonian $H_M = H_{ex} + H_A$ pertaining to $CoPt_3$ alloys. As its main contribution we assume classical Heisenberg-type isotropic exchange interactions H_{ex} within nearest-neighbour Co–Co and Co–Pt pairs. This simplified form seems sufficient as we are dealing only with the energetics of homogeneously magnetized states. The respective magnetic energies for Co–Co and Co–Pt pairs with parallel spins are $-JM_s^2$ and $-J'M_s^2$, respectively[5]. In addition, an anisotropy H_A connected with Co–Pt bonds, see (2), is included. Within first order perturbation theory the change in free energy due to H_M is given by an average of H_M over an unperturbed ensemble specified by the ψ_α. Mean-field calculations then yield

$$c_1 = J - 2J', \qquad c_2 = -2A/M_s^2. \tag{11}$$

In order to test the validity of the Landau approach based on the coupling (8) between structural and magnetic order and its prediction (9), we first focus on the anisotropy energy H_A (ignoring H_{ex}) and perform Monte Carlo simulations of the lattice model described before, but now under equilibrium conditions. The simulation box contains 43 200 atoms and is subjected to periodic boundary conditions in all three directions. Starting from disordered configurations, sufficient equilibration is achieved by performing runs up to 2×10^6 Monte Carlo steps, where two unlike atoms at arbitrary distance can be exchanged. For each temperature, averages were taken over six independent initial configurations. The location of the ordering transition in the field-free case is in agreement with literature data [16, 17]. In figure 3 the structural order parameter is plotted versus temperature, and indeed shows an increased transition temperature in the fully magnetized state in comparison to the zero field case. We have again used $A \simeq 225$ μeV (see above) which gives an increase of T_0 by 2 K. This increase favourably agrees with (9) when we set $c_1 = 0$ (see (11)) and $r_0/k_B \simeq 1$. These results show that with realistic parameters for the microscopic anisotropy energy a measurable shift in the ordering temperature is observed. The physical reason for the increase of T_0 in figure 3 is that through the presence of H_A the six nearest-neighbour sites of a Co atom with bond vectors not orthogonal to [111] become preferentially occupied by Pt atoms during the equilibration process, thus favouring the ordered structure. Basically this is the same mechanism that yields an increased structural anisotropy parameter P discussed before. Figure 3, therefore, provides additional evidence that H_A affects the ordering transition.

[5] Pt moments have been shown to depend on the actual atomic environment [14] but this effect is neglected here.

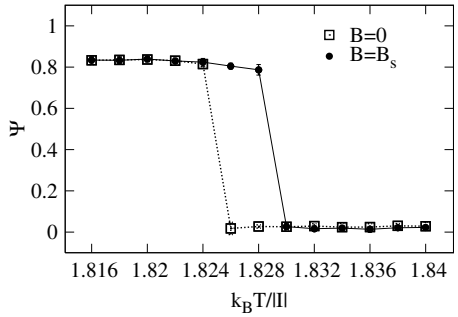

Figure 3. Simulated $L1_2$ order parameter $\Psi(T)$ for a bulk system at equilibrium as a function of temperature. Averages were performed over six realizations. Among the magnetic interactions only the anisotropy H_A has been included in the simulations. The upward shift of the ordering temperature $T_0(B) - T_0 \simeq 2$ K is clearly recognizable.

When exchange interactions are included, equation (9) predicts a much larger downward shift in T_0, which we can estimate now in a more quantitative manner. From [14] and known Co and Pt moments we obtain $JM_s^2 \simeq 140$ K and $J'M_s^2 \simeq 25$ K, while A is much smaller. Thus $(3c_1 + c_2)M_s^2/3 \simeq 90$ K, in agreement with the order of magnitude estimate of (9) given before, which was based on the comparison with measured Curie temperatures.

Again, the corresponding change in T_0 according to (9) can be compared with predictions from numerical computation. However, within a lattice model with nearest-neighbour chemical and isotropic exchange interactions, extra simulations for this problem are not actually needed when we note that in a fully magnetized sample the effect of H_{ex} is simply equivalent to modified chemical interactions

$$V'_{AA} = V_{AA} - JM_s^2; \qquad V'_{BB} = V_{BB}; \qquad V'_{AB} = V_{AB} - J'M_s^2. \tag{12}$$

Since the ordering transition temperature satisfies $k_B T_0 \simeq 1.83(V_{AA} + V_{BB} - 2V_{AB})/4$, we find, using (12), $k_B \Delta T_0(M_s) \simeq -1.83(J - 2J')M_s^2/4$. Because of (11) and $|c_2| \ll c_1$ this is consistent with (9) and establishes a semi-quantitative estimate $\Delta T_0(M_s) \simeq -41$ K. Clearly, since the exchange terms JM_s^2 and $J'M_s^2$ in (12) are relatively small, we could neglect them in our previous discussion of structural anisotropy.

Experimentally, for $CoPt_3$ it is probably very difficult to induce a sufficiently strong magnetization near T_0 such that the shift $\Delta T_0 \propto M^2$ becomes measurable. The situation is more favourable for $L1_0$ ordering of Co_xPt_{1-x} alloys near $x = 0.5$, where the Curie temperature is closer to the ordering temperature T_0 and even intersects with T_0 on the Co-rich side in the phase diagram. A similar situation occurs for Ni-rich Ni_xPt_{x-1} alloys [7]. For $L1_0$ ordering the structural part of the free energy f_S is again based on (6), but with a change in sign in w at $x = 1/2$, v sufficiently negative and additional stabilizing higher order terms [18]. Elastic energy contributions due to the tetragonal distortion in the $L1_0$ phase are thereby neglected. Coupling between structural order parameters and the magnetization can again be represented by equation (8). Considering magnetic fields $\mathbf{B} \parallel [001]$ we now obtain $\Delta T_{sp}(M) \simeq \Delta T_0(M) = -(c_1 + c_2)M^2/r_0$ and $\Delta T_C(\psi_{max}) = -(c_1 + c_2)/b_0$ instead of (9) and (10), with a measured value of about 10^2 K for the latter temperature shift. Using similar arguments as before, both temperature shifts $\Delta T_{sp}(M_s)$ and $\Delta T_c(\psi_{max})$ are expected to be of the same order.

5. Conclusions and outlook

Effects of external magnetic fields on both the far-from-equilibrium MBE growth of magnetic fcc alloys and their bulk structural phase behaviour at equilibrium have been studied. The statistical model we employed pertains to binary alloys of the $CoPt_3$ type and $L1_2$ ordering. KMC simulations are supplemented by equilibrium considerations based on Landau theory. Using realistic parameters for $CoPt_3$, our main aim was to explore the influence of the local crystalline magnetic anisotropy energy, modelled by a bond Hamiltonian H_A, on the structural properties of alloy nanoclusters, when a strong magnetic field is applied during growth. Such an effect, although small in $CoPt_3$, appears to be general and indeed leads to a notable enhancement of the structural anisotropy of the clusters and the associated PMA. Experimentally, in order to induce a large magnetization the substrate temperature should fall below the Curie temperature of disordered samples but at the same time remain in the known temperature window where PMA occurs.

More favourable conditions for studying these effects experimentally should exist for alloys like CoPt or FePt [19] undergoing $L1_0$ ordering, if clusters could be grown along the c-axis. As known from thin film measurements [20], the magnetic anisotropy in those alloys is a bulk property connected with alternating Co(Fe)- and Pt-rich layers caused by the $L1_0$ structural order. Hence, under growth conditions where $L1_0$ ordering is suppressed, one can expect a substantially larger field-induced PMA.

Acknowledgments

We thank M Albrecht and G Schatz for fruitful discussions. This work has been supported by the Deutsche Forschungsgemeinschaft DFG (SFB 513).

References

[1] Albrecht M, Maier A, Treubel F, Maret M, Poinsot P and Schatz G 2001 *Europhys. Lett.* **56** 884
[2] Albrecht M, Maret M, Maier A, Treubel F, Riedlinger B, Mazur U, Schatz G and Anders S 2002 *J. Appl. Phys.* **91** 8153
[3] Shapiro L, Rooney P W, Tran M Q, Hellman F, Ring K M, Kavanagh K L, Rellinghaus B and Weller D 1999 *Phys. Rev.* B **60** 12826
[4] Heinrichs S, Dieterich W and Maass P 2006 *Europhys. Lett.* **75** 167
[5] Heinrichs S, Dieterich W and Maass P 2006 Epitaxial growth of binary alloy nanostructures *Preprint* cond-mat/0607284
[6] Johnson M T, Bloemen P J H, den Broeder F J A and de Vries J J 1996 *Rep. Prog. Phys.* **59** 1409
[7] Cadeville M C and Morán-Lopéz J L 1987 *Phys. Rep.* **153** 331
[8] Binder K 1980 *Phys. Rev. Lett.* **45** 811
[9] Gauthier Y, Baudoing-Savois R, Bugnard J M, Bardi U and Atrei A 1992 *Surf. Sci.* **276** 1
[10] Bott M, Hohage M, Morgenstern M, Michely T and Comsa G 1996 *Phys. Rev. Lett.* **76** 1304
[11] Einax M, Heinrichs S, Maass P, Majhofer A and Dieterich W 2007 *Proc. E-MRS 2006 Spring Meeting (Nice)*; *Mater. Sci. Eng.* C at press
[12] Chikazumi S and Graham C D 1999 *Physics of Ferromagnetism* 2nd edn (Oxford: Oxford University Press)
[13] Dang M Z and Rancourt D G 1996 *Phys. Rev.* B **53** 2291
[14] Sanchez J M, Morán-López J L, Leroux C and Cadeville M C 1989 *J. Phys.: Condens. Matter* **1** 491
[15] Lai Z W 1990 *Phys. Rev.* B **41** 9239
[16] Frontera C, Vives E, Castán T and Planes A 1997 *Phys. Rev.* B **55** 212
[17] Kessler M, Dieterich W and Majhofer A 2001 *Phys. Rev.* B **64** 125412
Kessler M, Dieterich W and Majhofer A 2003 *Phys. Rev.* B **67** 134201
[18] Tanoğlu G B, Braun R J, Cahn J W and McFadden G B 2003 *Interfaces Free Boundaries* **5** 275
[19] Massalski T 1996 *Binary Alloy Phase Diagrams* vol 2 (Metals Park, OH: ASM International)
[20] Iwata S, Yamashita S and Tsunashima S 1997 *IEEE Trans. Magn.* **33** 3670